A modeling based evaluation of isothermal rebreathing for breath gas analyses of highly soluble volatile organic compounds

J. King, K. Unterkofler, H. Koc, A. Kupferthaler,
G. Teschl, S. Teschl, H. Hinterhuber, A. Amann

Technical Report, Breath Research Institute of the Austrian Academy of Sciences
April 2010

1 Abstract

Over the past decade, much advance has been made for exploiting the diagnostic and metabolic information encapsulated in a number of endogenous volatile organic compounds appearing in human exhaled breath. However, our causal understanding of the relationships between breath concentrations of such trace gases and their underlying systemic levels clearly lags behind the enormous analytical progress in this field. In particular, formal means for evaluating the information content and predictive power of various sampling regimes are still lacking.
Here, we focus on isothermal rebreathing which has been proposed as an experimental technique for estimating the *alveolar* levels of hydrophilic VOCs in exhaled breath. Using the prototypic test compound acetone we demonstrate that the end-tidal breath profiles of such substances during isothermal rebreathing show characteristics that contradict the conventional pulmonary inert gas elimination theory due to Farhi. On the other hand, these profiles can reliably be captured by virtue of a previously developed mathematical model for the general exhalation kinetics of highly soluble, blood-borne VOCs, which explicitly takes into account airway gas exchange as major determinant of the observable breath output. This model allows for a mechanistic analysis of various rebreathing protocols suggested in the literature. In particular, it clarifies the discrepancies between *in vitro* and measured blood:breath ratios of hydrophilic VOCs and yields further quantitative insights into the physiological components of isothermal rebreathing.

2 Introduction

Recently, several efforts have been undertaken to complement measurements of volatile organic compounds occurring in human breath with adequate physical models mapping substance-specific distribution mechanisms in the pulmonary tract as well as in the body tissues [1, 18, 20, 24]. Such mechanistic descriptions of the observable exhalation kinetics will not only contribute to a better understanding regarding the relevance of the extracted breath concentration with respect to the endogenous situation (i.e., with respect to blood or tissue concentrations, which in turn can be seen as the decisive quantities for diagnostic decisions) but might also serve as valuable tools for evaluating the information content and predictive power of various experimental regimes. Some major breath compounds have already been investigated in this form, e.g., during exercise conditions or exposure scenarios. Within this context, the main focus of this article will be on a modeling based review of isothermal rebreathing, which has been proposed as an experimental technique for estimating the *alveolar* levels of hydrophilic exhaled trace gases [15, 27]. This class of compounds has been demonstrated to significantly interact with the water-like mucus membrane lining the conductive airways, an effect which has become known as wash-in/wash-out behavior. For further details we refer to [1, 2]. As a phenomenological consequence, exhaled breath concentrations of such highly water soluble substances tend to be diminished on their way up from the deeper respiratory tract to the airway opening. The resulting discrepancies between the "true"

alveolar and the measured breath concentration can be substantial (even if breath samples are drawn in a strictly standardized manner employing, e.g., CO_2- or flow-controlled sampling) and will depend on a variety of factors, such as airway temperature profiles and airway perfusion as well as breathing patterns.

In particular, the above-mentioned effect considerably departs from the classical Farhi description of pulmonary inert gas exchange [7], on the basis of which the conventional dogma has been established that end-tidal air will reflect the alveolar level and that arterial concentrations can be assessed by simply multiplying this value with the blood:gas partition coefficient $\lambda_{\mathrm{b:air}}$ at body temperature. This "common knowledge" has first been put into question in the field of breath alcohol testing, revealing *observable* blood-breath concentration ratios of ethanol during tidal breathing that are unexpectedly high compared to the partition coefficient derived in vitro [15]. Similarly, excretion data (defined as the ratio between steady state partial pressures in expired air and mixed venous blood) of highly water soluble compounds (including the MIGET test gas acetone) have been shown to underestimate the values anticipated by treating the airways as an inert tube [3,35].

In a previously published mathematical model for the breath gas dynamics of highly soluble trace gases, airway gas exchange is taken into account by separating the lungs into a bronchial and alveolar compartment, interacting via a diffusion barrier mimicking pre- and post-alveolar uptake [18]. This formulation has proven its ability to reliably capture both end-tidal breath profiles as well as systemic dynamics of acetone in a variety of experimental situations and will be used here for illuminating the physiological processes underlying isothermal rebreathing tests as carried out in the literature. For comparative reasons, the illustration here will mainly be limited to acetone, with possible extrapolations of our findings to other highly soluble VOCs indicated where appropriate.

3 Methods

3.1 Experiments

Extensive details regarding the experimental input of our investigations are given elsewhere [17,18]. Here, we will only briefly discuss the parts of the setup relevant for the present context. In particular, all results presented in the sequel were obtained in conformity with the Declaration of Helsinki and with the necessary approvals by the Ethics Commission of Innsbruck Medical University.

The rebreathing system itself consists of a Tedlar bag with volume $\tilde{V}_{\mathrm{bag}} = 3$ l that can directly be connected to a spirometer headmask, from which end-tidal exhalation segments are drawn into a Proton Transfer Reaction Mass Spectrometer (PTR-MS; Ionicon Analytik GmbH, Innsbruck, Austria) as described in [17]. The bag is warmed to 37 ± 1 °C using a specially designed outer heating bag (Infroheat Ltd., Wolverhampton, UK) as described in [26]. This is intended to assist the thermal equilibration between the alveolar tract and the upper airways as well as to prevent condensation and subsequent losses of hydrophilic VOCs depositing onto water droplets forming on the surface wall of the bag. End-tidal acetone concentrations were determined by monitoring its protonated form at $m/z = 59$ (dwell time: 200 ms). Additionally, we routinely measure the mass-to-charge ratios $m/z = 21$ (isotopologue of the primary hydronium ions used for normalization; dwell time: 500 ms), $m/z = 37$ (first monohydrate cluster for estimating sample humidity; dwell time: 2 ms), $m/z = 69$ (protonated isoprene; dwell time: 200 ms), $m/z = 33$ (protonated methanol; dwell time: 200 ms) as well as the parasitic precursor ions NH_4^+ and O_2^+ at $m/z = 18$ and $m/z = 32$, respectively, with dwell times of 10 ms each. In particular, the pseudo concentrations associated with $m/z = 32$ determined according to the standard conversion formula (1) in [29] will be used as an indicator for the end-tidal partial partial pressure P_{O_2} of oxygen, relative to an assumed nominal steady state level at rest of about 100 mmHg. Similarly, calibrated pseudo concentrations corresponding to $m/z = 37$ are considered as surrogates for absolute sample humidity C_{water} [18]. Partial pressures P_{CO_2} of carbon dioxide are obtained via a separate sensor. Table 1 summarizes the measured quantities used in this paper. In general, breath concentrations will always refer to end-tidal levels. Moreover, an underlying sampling interval of 5 s is applied for each variable.

Variable	Symbol	Nominal value (units)
Cardiac output	$\dot{Q}_{\mathrm{c}}$	6 (l/min) [23]
Alveolar ventilation	$\dot{V}_{\mathrm{A}}$	5.2 (l/min) [33]
Acetone concentration	C_{measured}	1 (μg/l) [30]
CO_2 partial pressure	$P_{\mathrm{CO_2}}$	40 (mmHg) [21]
Water content	C_{water}	4.7 (%) [12]
O_2 partial pressure	$P_{\mathrm{O_2}}$	100 (mmHg) [21]

Table 1: Summary of measured parameters together with some nominal literature values during rest, assuming ambient conditions; breath concentrations refer to end-tidal levels.

3.2 Physiological model

For the sake of completeness, the model structure is presented in Fig. 1, while for the associated compartmental mass balance equations we refer to the appendix and the original publication [18]. The body is divided into four distinct functional units, for which the underlying concentration dynamics of the VOC under scrutiny will be taken into account: bronchial/mucosal compartment (C_{bro}; gas exchange), alveolar/end-capillary compartment (C_{A}; gas exchange), liver (C_{liv}; production and metabolism) and tissue (C_{tis}; storage). The nomenclature is detailed in the legend of Fig. 1.

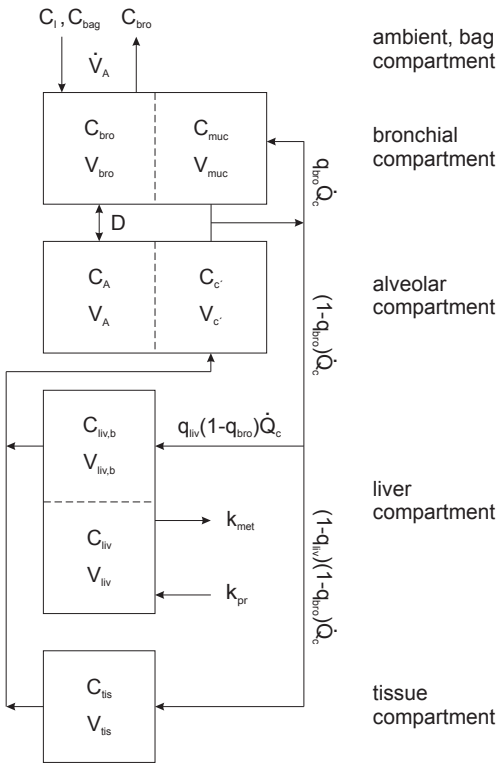

Figure 1: Sketch of the model structure used for capturing dynamic VOC concentrations C. Subscripts connote as follows: bag, *rebreathing bag*; I, *inhaled*; bro, *bronchial*; muc, *mucosal*; A, *alveolar*; c′, *end-capillary*; liv, *liver*; tis, *tissue*; b, *blood*. Dashed boundaries indicate a diffusion equilibrium, governed by the respective partition coefficients λ, e.g., $\lambda_{\mathrm{muc:air}}$.

Moreover, the measurement process is described by

$$C_{\text{measured}} = C_{\text{bro}}, \tag{1}$$

i.e., we assume that measured (end-tidal) breath concentrations reflect the bronchial levels.
In particular, for highly water and blood soluble compounds such as acetone the present model replaces the familiar Farhi equation

$$C^{\text{F}}_{\text{measured}} = C_{\text{A}} = \frac{\frac{\dot{V}_{\text{A}}}{\dot{Q}_{\text{c}}} C_{\text{I}} + C_{\bar{\text{v}}}}{\lambda_{\text{b:air}} + \frac{\dot{V}_{\text{A}}}{\dot{Q}_{\text{c}}}} = \frac{C_{\text{a}}}{\lambda_{\text{b:air}}}, \tag{2}$$

describing the steady state relationship between inhaled (ambient) concentration C_{I}, measured breath concentration $C^{\text{F}}_{\text{measured}}$, mixed venous concentration $C_{\bar{\text{v}}}$ and arterial concentration C_{a} during tidal breathing with the expression

$$C_{\text{measured}} = C_{\text{bro}} = \frac{r_{\text{bro}} C_{\text{I}} + (1 - q_{\text{bro}}) C_{\bar{\text{v}}}}{(1 - q_{\text{bro}}) \frac{\lambda_{\text{muc:air}}}{\lambda_{\text{muc:b}}} + r_{\text{bro}}} = \frac{r_{\text{bro}} C_{\text{I}} + C_{\text{a}}}{\frac{\lambda_{\text{muc:air}}}{\lambda_{\text{muc:b}}} + r_{\text{bro}}}. \tag{3}$$

Here, $q_{\text{bro}} \leq 1$ is an estimate of the effective fractional bronchial perfusion (which might be substance-specific), while

$$r_{\text{bro}} = \frac{\dot{V}_{\text{A}}}{q_{\text{bro}} \dot{Q}_{\text{c}}}$$

denotes the *bronchial* ventilation-perfusion ratio.

An explicit temperature dependence of airway gas exchange is incorporated into the model via the mucosa:air partition coefficient $\lambda_{\text{muc:air}} = \lambda_{\text{muc:air}}(\bar{T})$, varying according to a characteristic mean airway and bronchial blood temperature $\bar{T}$ (in °C). Specifically, the latter has been shown to be accessible by virtue of the measured sample humidity C_{water} (see [18]). Furthermore it is assumed that the solubilities in bronchial blood and the mucus layer are proportional over the temperature range considered, with the proportionality constant given by

$$\lambda_{\text{muc:b}} := \lambda_{\text{muc:air}}(37\ ^\circ\text{C}) / \lambda_{\text{b:air}}(37\ ^\circ\text{C}). \tag{4}$$

As a first approximation, the mucosa layer can be assumed to inherit the physico-chemical properties of water. In particular, $\lambda_{\text{muc:air}}$ will properly be reflected by the respective substance-specific water:air partition coefficient, which is usually available from the literature (see, e.g., the compendium in [32]).

A central role is played by the gas exchange location parameter D, mimicking pre- and post-alveolar uptake in the mucosa. As has been discussed in [18], for highly water soluble substances D is close to zero during rest and will increase with ventilation. Here, we will model this dependency as

$$D(\dot{V}_{\text{A}}) := k_{\text{diff}} \max\{0, \dot{V}_{\text{A}} - \dot{V}^{\text{rest}}_{\text{A}}\},\ k_{\text{diff}} \geq 0. \tag{5}$$

Again, k_{diff} constitutes an a priori unknown value that will have to be estimated from experimental data.

3.3 Heuristic considerations

As has already been indicated in the introduction, Equation (2) is insufficient for capturing experimentally obtained arterial blood-breath concentration ratios (BBR) of highly water soluble trace gases during free breathing at rest (i.e., assuming $C_{\text{I}} = 0$). For instance, in the specific case of acetone, multiplying the proposed population mean of approximately 1 μg/l [30] in end-tidal breath with a blood:gas partition coefficient of $\lambda_{\text{b:air}} = 340$ [4] at body temperature appears to grossly underestimate arterial blood levels spreading around 1 mg/l [16, 34].

In contrast, Equation (3) asserts that the observable arterial blood-breath ratio is

$$\mathrm{BBR} = \frac{C_\mathrm{a}}{C_\mathrm{measured}} = \lambda_\mathrm{muc:air}(\bar{T})/\lambda_\mathrm{muc:b} + r_\mathrm{bro} \quad (\geq \lambda_\mathrm{b:air}) \tag{6}$$

and will thus depend on airway temperature and airway blood flow as mentioned in the previous paragraph. From the last expression it is clear that the higher (water) soluble a VOC under scrutiny, the more drastically its observable BBR will be affected by the current airway temperature, with an inverse relation between these two quantities. This deduction is consistent with measurements by Ohlsson et al. [27] conducted in the field of alcohol breath tests, reporting a monotonous decrease of BBR values for ethanol with increasing exhaled breath temperature. In the same contribution, BBRs of ethanol during normal tidal breathing were shown to typically exceed a value of 2500, which differs from the expected value $\lambda_\mathrm{b:air} = 1756$ by more than 40 %. For perspective, assuming a mean characteristic airway temperature of $\bar{T} = 34$ °C during free tidal breathing, based on Equations (4) and (6) as well as on the values for $\lambda_\mathrm{muc:air}$ given in [32], we predict an experimentally observable blood-breath ratio of ethanol ≥ 2300. On the other hand, blood-breath ratios of less soluble VOCs, e.g., acetone, will additionally be affected by the comparatively large value of r_bro, which stems from the diffusion disequilibrium between the alveolar and bronchial space.

Apart from providing some experimental evidence for the validity of Equation (3), these ad hoc calculations suggest that the common practice of multiplying the measured breath concentration C_measured with the in vitro blood:air partition coefficient $\lambda_\mathrm{b:air}$ to obtain endogenous arterial concentrations for highly water soluble gases will result in an estimation that might drastically differ from the true blood level.

In the following we will review isothermal rebreathing as a valuable method for removing the aforementioned discrepancies. The heuristic intention leading to isothermal rebreathing is to create an experimental situation where the alveolar levels of highly soluble VOCs are not altered during exhalation due to loss of such substances to the cooler mucus layer of the airways. This can be accomplished by "closing the respiratory loop", i.e., by continuous re-inspiration and -expiration of a fixed mass of air from a rebreathing receptacle (e.g., a Tedlar bag), causing the airstream to equilibrate with the mucosa linings over the entire respiratory cycle [4, 26, 27]. Additionally, warming the rebreathing volume to body temperature (hence isothermal) will ensure similar solubilities of these VOCs in both regions, alveoli and airways.
Formally, a model capturing the experimental situation during isothermal rebreathing can simply be derived by augmenting the previous model equations with an additional compartment representing the rebreathing receptacle, i.e.,

$$\frac{\mathrm{d}C_\mathrm{bag}}{\mathrm{d}t}\tilde{V}_\mathrm{bag} = \dot{V}_\mathrm{A}(C_\mathrm{bro} - C_\mathrm{bag}) \tag{7}$$

and setting $C_\mathrm{I} = C_\mathrm{bag}$. Following the line of argument in Section 3.2.3 of [18], it can easily be checked that all fundamental system properties discussed there remain valid. In particular, if we assume that the conducting airways are warmed to body temperature, i.e.,

$$\frac{\lambda_\mathrm{muc:air}}{\lambda_\mathrm{muc:b}} \to \frac{\lambda_\mathrm{muc:air}(37\ ^\circ\mathrm{C})}{\lambda_\mathrm{muc:b}} = \lambda_\mathrm{b:air} \tag{8}$$

as temperature increases, we may conclude that the compartmental concentrations will tend to a globally asymptotically stable steady state obeying

$$C^\mathrm{rebr}_\mathrm{measured} = C^\mathrm{rebr}_\mathrm{bro} = C^\mathrm{rebr}_\mathrm{bag} = C^\mathrm{rebr}_\mathrm{A} = \frac{C^\mathrm{rebr}_{\bar{\mathrm{v}}}}{\lambda_\mathrm{b:air}} = \frac{C^\mathrm{rebr}_\mathrm{a}}{\lambda_\mathrm{b:air}}. \tag{9}$$

This is a simple consequence of substituting C_I with C_bro in Equation (3) according to the steady state relation associated with Equation (7). Note that if steady state conditions hold they will depend solely on the blood:air partition coefficient $\lambda_\mathrm{b:air}$ at 37 °C, rendering isothermal rebreathing as an extremely stable technique for providing a reproducible coupling between breath and endogenous (blood) levels. Particularly, it theoretically avoids the additional measurement of ventilation- and perfusion-related variables that would otherwise affect this relationship, thereby significantly simplifying the required technical

setup for breath sampling. However, as will be illustrated in the following, the major practical obstacle is to guarantee that such a steady state is effectively attained.

For comparative reasons, it should also be pointed out that if $C_{\bar{\mathrm{v}}}^{\mathrm{rebr}} \approx C_{\bar{\mathrm{v}}}$, i.e., if the mixed venous concentrations stay constant during rebreathing (which – at least in the first phase of rebreathing – can be justified to some extent by reference to tissue lung transport delays of the systemic circulation [10]), then the ratios between measured rebreathing concentrations and end-tidal concentrations during free breathing at rest are predicted to follow an entirely different trend according to Equation (2) and Equation (3) (see also Fig. 2). To this end, note that while in the first case we find that

$$\frac{C_{\mathrm{measured}}^{\mathrm{F,rebr}}}{C_{\mathrm{measured}}^{\mathrm{F,free}}} := \frac{C_{\mathrm{measured}}^{\mathrm{F}}|_{C_{\mathrm{I}}=C_{\mathrm{bag}}}}{C_{\mathrm{measured}}^{\mathrm{F}}|_{C_{\mathrm{I}}=0}} \rightarrow \frac{\lambda_{\mathrm{b:air}} + \frac{\dot{V}_{\mathrm{A}}}{\dot{Q}_{\mathrm{c}}}}{\lambda_{\mathrm{b:air}}}, \tag{10}$$

the present model yields

$$\frac{C_{\mathrm{measured}}^{\mathrm{rebr}}}{C_{\mathrm{measured}}^{\mathrm{free}}} \rightarrow \frac{(1-q_{\mathrm{bro}})\frac{\lambda_{\mathrm{muc:air}}}{\lambda_{\mathrm{muc:b}}} + r_{\mathrm{bro}}}{(1-q_{\mathrm{bro}})\lambda_{\mathrm{b:air}}}. \tag{11}$$

For highly soluble trace gases, this observation constitutes a simple test for assessing the adequacy of the Farhi formulation regarding its ability to describe the corresponding exhalation kinetics. Indeed, for sufficiently large $\lambda_{\mathrm{b:air}}$, the right-hand side of Equation (10) will be close to one, while the right-hand side of Equation (11) suggests that rebreathing should cause the associated breath concentrations to increase. In other words, for this class of compounds a non-constant behavior during the initial isothermal rebreathing period indicates that Equation (2) will fail to capture some fundamental characteristics of pulmonary excretion. Such tests are of particular importance in the context of endogenous MIGET methodology (Multiple Inert Gas Elimination Technique, based on endogenous rather than externally administered VOCs [3]) and might potentially be used for detecting deviations of the proposed test gases from the underlying Farhi description.

4 Results

4.1 Single rebreathing

In this section we will discuss some simulations and preliminary experiments conducted in order to study the predictive value of isothermal rebreathing within a realistic setting. For this purpose we will first mimic isothermal rebreathing as it has been carried out in various investigations [26,27]. We assume that $\tilde{V}_{\mathrm{bag}} = 3$ l according to Section 3.1.

Fig. 2 shows typical profiles of breath acetone, water, CO_2 and oxygen content as well as cardiac output during normal breathing and isothermal rebreathing at rest (starting after 1.5 minutes of quiet tidal breathing and ending at approximately 3.7 min). In particular, these data correspond to one single normal healthy volunteer. As has been explained in Section 3.1, P_{O_2} is derived by scaling the end-tidal steady state of the pseudo concentration at $m/z = 32$ to a basal value of 100 mmHg during free breathing. Rebreathing was instituted by inhaling to total lung capacity and exhaling until the bag was filled, thereby providing an initial bag concentration which can be assumed to resemble the normal end-exhaled steady state, i.e.,

$$C_{\mathrm{bag}}(0) = C_{\mathrm{bro}}(0). \tag{12}$$

Rebreathing was then continued until either the individual breathing limit was reached or the CO_2 concentrations increased above 55 mmHg. Due to the fact that our spirometer system works on the basis of differential pressure with respect to ambient air, alveolar ventilation $\dot{V}_{\mathrm{A}}$ could not reliably be measured during the rebreathing period. However, this quantity can be simulated on the basis of monitored values for end-tidal CO_2 and O_2 as follows. Under iso-oxic conditions, after a certain threshold value has been

exceeded, ventilation is known to increase linearly with alveolar carbon dioxide partial pressure. Moreover, the corresponding slopes (reflecting the chemoreflex sensitivity of breathing) are dependent on the current alveolar oxygen partial pressure (see also [21]). Here, it is assumed that alveolar levels reflect those of the peripheral and central chemoreceptor environment. Hypoxia during rebreathing enhances chemoreflex sensitivity, therefore resulting in a hyperbolic relation between the mentioned slopes and alveolar oxygen partial pressures. These findings yield a simple model capturing the chemoreflex control of breathing in humans [6, 22], which has been re-implemented here in order to compute $\dot{V}_{\mathrm{A}}$ from basal values during free breathing as shown in Fig. 2, fourth panel.

For identifiability reasons, the rate constant k_{met} describing linear acetone metabolism in the liver is set to fixed value of $k_{\mathrm{met}} = 0.18\,\mathrm{l/min}$ [18]. This completes the necessary data for simulating the aforementioned rebreathing experiment. More specifically, the model response in the first panel is computed by solving the standard ordinary least squares problem

$$\underset{\boldsymbol{\theta}}{\operatorname{argmin}} \sum_{i=0}^{n} \big(y_i - C_{\mathrm{bro}}(t_i)\big)^2, \quad \text{s.t.} \begin{cases} g(\boldsymbol{u}_0, \boldsymbol{\theta}) = 0 & \text{(steady state)} \\ \boldsymbol{\theta} \geq 0 & \text{(positivity)} \\ q_{\mathrm{bro}} \leq 1 & \text{(normalization)} \\ C_{\mathrm{bag}}(0) = C_{\mathrm{bro}}(0) & \text{(initial bag concentration)} \end{cases}$$

with respect to the unknown vector $\boldsymbol{\theta} := (\boldsymbol{c}_0, k_{\mathrm{pr}}, k_{\mathrm{diff}}, q_{\mathrm{bro}})$ by means of a multiple shooting algorithm as discussed in [18]. Here, y_i denotes the measured breath data at time instant t_i ($t_0 = 0$) and g is the right hand side of the corresponding ODE mass balance system. Moreover, $\boldsymbol{c}_0$ and $\boldsymbol{u}$ lump together the (partially) unknown intial conditions $\boldsymbol{c}_0 = (C_{\mathrm{bag}}(0), C_{\mathrm{bro}}(0), C_{\mathrm{A}}(0), C_{\mathrm{liv}}(0), C_{\mathrm{tis}}(0))$ and the measured input variables $\boldsymbol{u} = (\dot{Q}_{\mathrm{c}}, \dot{V}_{\mathrm{A}}, C_{\mathrm{water}})$, respectively.

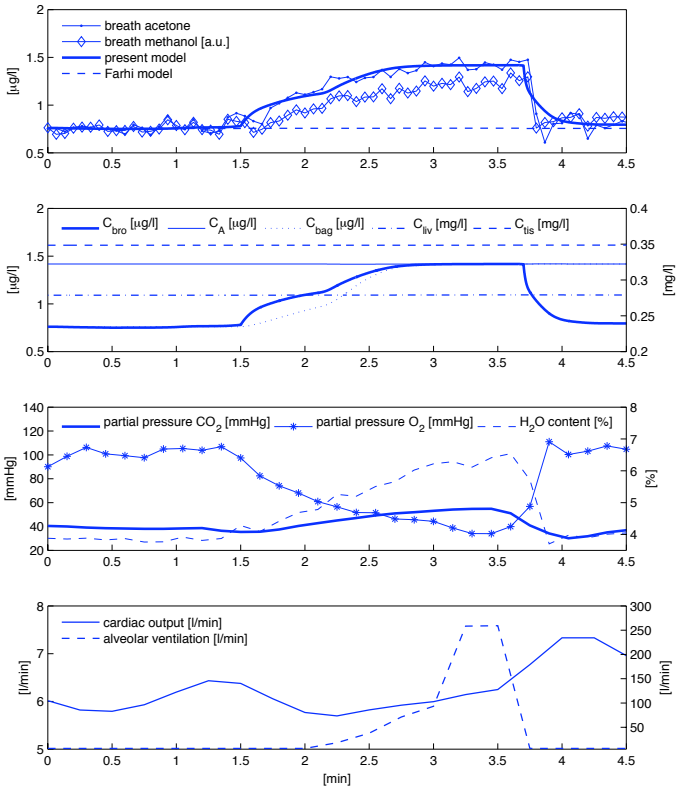

Figure 2: Representative outcome of an isothermal rebreathing experiment during rest. Data correspond to one single normal healthy volunteer. Isothermal rebreathing starts after 1.5 minutes of quiet tidal breathing and ends at approximately 3.7 min.

From the previous figure, the fitted model is found to faithfully reproduce the observed data, which extends the range of experimental situations for which the underlying formalism has been validated. In contrast, as may have been anticipated from Equation (10), the classical Farhi model fails to capture the given breath profile. Considering the fact that the latter model is included in our present formulation as a limiting case for $q_{\mathrm{bro}} = 0$ and $D \to \infty$ [18], its associated output can again computed by solving an ordinary least squares problem similar to the one presented above.
In particular, the presented data appear to consolidate the heuristic considerations in Section 3.3 and confirm that the alveolar concentration of acetone during free tidal breathing will differ from the associated bronchial (i.e., measured end-exhaled) level by a factor of up to 2. This is due to an effective diffusion disequilibrium between the conducting airways and the alveolar space. During isothermal rebreathing, this barrier slowly vanishes and causes the measured breath concentration to approach the underlying alveolar concentration (which itself stays relatively constant during this phase). We stress the fact that in order to simulate a similar response by using the conventional Farhi model, one essentially would have to postulate a temporarily increased endogenous acetone production during rebreathing, which evidently lacks physiological plausibility. For comparative reasons, in addition we provide the dynamic response of breath methanol, scaled to match the initial level of breath acetone. Taking into account a methanol blood:gas partition coefficient of $\lambda_{\mathrm{b:air}} = 2590$ at body temperature [20], from Equation (11) it can be deduced that for this compound the differences between concentrations extracted during free breathing and rebreathing primarily stem from the thermal equilibration between airways and alveolar tract as

indicated in Equation (8). The associated rise in temperature is mirrored by an increase of sample water vapor C_{water} until approaching an alveolar level of about 6.2 %, which is of similar order like comparable data in the literature [26]. In particular, the previously presented profile of methanol shows the necessity of including an explicit temperature dependence in models describing the breath profiles of highly soluble VOCs.
The visually convincing fit in Fig. 2 was further investigated by residual analysis. Residual plots versus time and model predictions reveal random patterns, thereby suggesting that the assumptions of independent, additive and homoscedastic error terms underlying ordinary least squares methodology are reasonable. No statistically significant autocorrelation among the residuals could be detected. As a result of these ad hoc tests, we conclude that the residuals are interchangeable, which offers the possibility to construct bootstrap confidence intervals for assessing the uncertainty level associated with the above estimates [13, 31]. Bootstrapping (BS) appears to be particularly suitable in this context, as it heavily relies on extensive resampling of high frequency process data, the latter one being a natural characteristic of breath gas analytical investigations.

Variable	Symbol	Fitted value (units)	BS 95 % CIs
Fractional bronchial blood flow	q_{bro}	0.0052	(0.0044,0.0059)
Diffusion constant Eq. (5)	k_{diff}	1.2	(0.34,4.77)
Endogenous acetone production	k_{pr}	91.54 (μg/min)	(89.23,94.7)
Initial concentration bronchioles	$C_{\text{bro}}(0)$	0.76 (μg/l)	(0.74,0.79)
Initial concentration alveoli	$C_{\text{A}}(0)$	1.42 (μg/l)	(1.38,1.47)
Initial concentration liver	$C_{\text{liv}}(0)$	0.28 (mg/l)	(0.27,0.29)
Initial concentration tissue	$C_{\text{tis}}(0)$	0.35 (mg/l)	(0.34,0.36)

Table 2: Decisive model parameters associated with the fit in Fig. 2 and corresponding bootstrap percentile confidence intervals.

The confidence intervals in Table 2 suggest that under the previous assumptions and constraints all unknown parameters and initial conditions except k_{diff} can be determined from the acetone breath profile with reasonable accuracy. The relatively poor estimability of k_{diff} within the experimental framework presented here can mainly be ascribed to the low sensitivity of the observable breath concentration with respect to this parameter (as can be deduced by computing the partial derivatives of the model output with respect to k_{diff}, e.g., by solving the associated variational equations [11]). This problem might be circumvented by designing multi-experimental regimes guaranteeing a sufficiently large and independent influence of all parameters to be determined (e.g., rebreathing followed by a hyperventilation or moderate exercise scenario as described in [18]).

While the preceding considerations suggest that inference on endogenous acetone kinetics by virtue of exhaled breath measurements during isothermal rebreathing is potentially feasible, it should be emphasized that the extracted values are clearly model-dependent. Moreover, further experimental evidence needs to be gathered before such estimates can become practically relevant, particularly with respect to distinct populations anticipated to provide characteristic experimental outcomes in response to the measurement regime indicated above. In this context, it would be particularly interesting to determine the impact of pathologies that are known to alter bronchial blood flow (such as asthma or bronchiectasis) on the results of isothermal rebreathing tests. Summarizing, the presented analysis should merely be seen as a preliminary proof of concept, that primarily aims at clarifying the physiological mechanisms affecting the breath levels of highly soluble VOCs during isothermal rebreathing.

4.2 Cyclic rebreathing

On the basis of the parameter values extracted in the previous subsection, in the following we will briefly discuss a sequential rebreathing protocol developed by O'Hara et al. [26], which aims at improving the

patient compliance of conventional rebreathing by repeatedly providing cycles of five rebreaths with intermediate periods of free tidal breathing lasting approximately 10 minutes. Isothermal rebreathing is instituted after 10 minutes of rest, again by inhaling to total lung capacity and exhaling to residual volume into a Tedlar bag with volume $\tilde{V}_{\mathrm{bag}} = 3$ l. After each rebreathing cycle, the bag is closed, a small amount of bag air is measured and the volunteer starts the next cycle by exhaling to residual volume and inhaling from the bag. From Fig. 2 we assume that all input variables $\boldsymbol{u}$ will have returned to pre-rebreathing values within the 10 minutes breaks and that their behavior during the individual rebreathing segments (postulated to last 0.5 minutes) will correspond to the profiles presented in Fig. 2. In particular, as a drastic change of cardiac output could not be observed in the rebreathing phase (see also [26]), we fix its value at an initial level of 6 l/min. Values for the initial conditions $\boldsymbol{c}_0$ as well as for the additional parameters are adopted from the previous section. These premises allow us to simulate repeated rebreathing as displayed in Fig. 3. The initial bag concentration at the onset of each individual rebreathing cycle is determined by the final bag concentration after the preceding rebreathing cycle, i.e., no fresh room air enters the bag according to the experimental protocol described in [26].

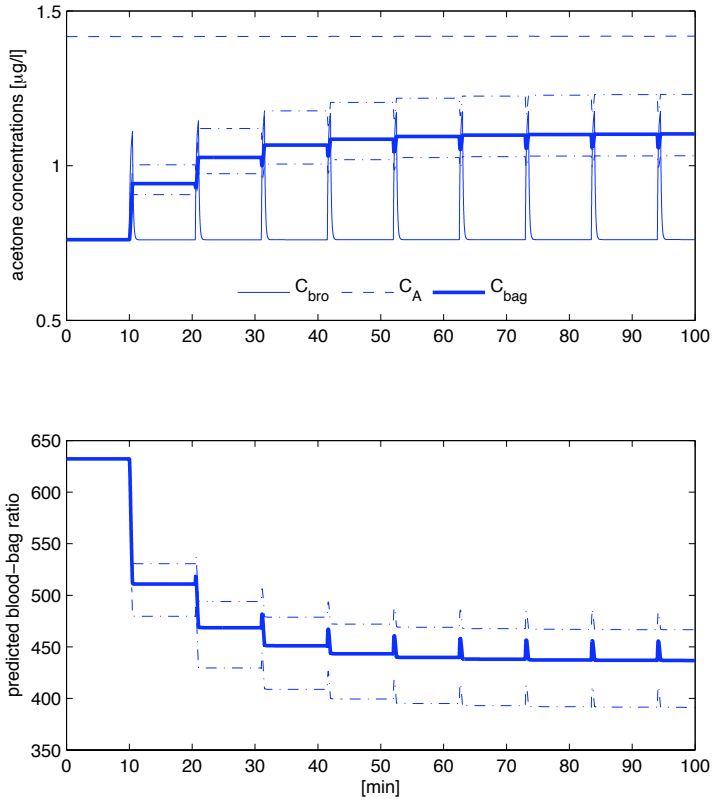

Figure 3: Simulation of a cyclic rebreathing protocol with intermediate pauses of 10 minutes characterized by free tidal breathing. Dash-dotted lines represent upper and lower bounds for the bag concentration as well as for the observable blood-bag ratio. These bounds were obtained by assuming that the airway temperature either instantaneously rises to body core temperature or remains constant during the individual rebreathing periods.

The bag concentration profile in Fig. 3 qualitatively resembles the data presented by O'Hara et al.. However, what emerges from this modeling-based analysis is that in spite of steadily increasing bag

concentrations (finally reaching a plateau level), the latter do not necessarily approach the underlying alveolar concentration as in the case of single cycle rebreathing. The major reason for this is a lack of thermal and diffusional equilibration between airways and alveolar region within the individual rebreathing segments. One potential way to circumvent this problem might be to reduce the desaturation and cooling of the airway tissues between consecutive rebreathing segments by keeping the intermediate time interval of free tidal breathing as short as possible while simultaneously maintaining a regime allowing comfortable breathing. The second panel in Fig. 3 displays the evolution of predicted blood-bag concentration ratios during the course of experimentation. Note that the in vitro blood:gas partition coefficient $\lambda_{\mathrm{b:air}} = 340$ is never attained. This can offer some explanation for the discrepancies that continue to exist with regard to theoretical and observed ratios between blood and (rebreathed) breath levels [25]. The final plateau value and the observable BBR of acetone will vary with temperature as shown in Fig. 3, which is consistent with similar observations made in the case of breath ethanol measurements [27].

5 Discussion

Here we have successfully applied a previously published compartment model for the exhalation kinetics of highly soluble, blood-borne VOCs to the experimental framework of isothermal rebreathing. The proposed model has proven sufficiently flexible to capture the associated end-tidal breath dynamics of acetone, which can be viewed as a prototypical test compound within this context. Data are presented for one single representative subject only, inasmuch as our main emphasis lay on describing the fundamental features of observable VOC behavior within the above-mentioned experimental regime. Some important practical implications emerge from this analysis. Firstly, it is demonstrated that the classical Farhi setting will fail to reproduce the experimentally measured data if a constant endogenous production and metabolism rate is postulated. This is due to the fact that airway gas exchange, being a major determinant affecting breath concentration profiles during isothermal rebreathing, is not taken into account within this formalism.

From an operational point of view our data indicate that even if isothermal rebreathing is carried out until the individual breathing limit is reached, a steady state according to Equation (9) might not necessarily be attained for highly soluble blood-borne VOCs. In particular, it has been shown in the case of acetone that end-exhaled breath (or bag) concentrations extracted after about 0.5 min of rebreathing (corresponding to the common protocol of providing around five consecutive rebreaths) are still likely to underestimate the underlying alveolar level, as do end-exhaled levels during free tidal breathing. While the alveolar concentration might be extrapolated to some extent from *partially* rebreathed breath volumes by employing parameter estimation procedures as outlined above, adequate rebreathing setups allowing for longer and more tolerable experiments will necessarily hinge on the continuous removal of CO_2 and on the replacement of metabolically consumed oxygen (see also closed chamber techniques as discussed in [8]). The influence of chemical binding agents for CO_2 (e.g., "soda lime") used for this purpose on the measured breath and bag concentrations remains to be settled. Furthermore, we stress the fact that systemic blood levels themselves will change in the course of rebreathing due to feedback from the body tissues. While this is not expected to be a major issue for rebreathing periods less than one minute (taking into account the tissue-lung transport delays of the systemic circulation), one has to bear in mind that the alveolar concentration extracted from a fully equilibrated rebreathing sample will generally reflect a mixed venous concentration that is distinct from the steady state level during free breathing. The associated deviation will depend on substance-specific distribution processes within the body. For perspective, these dynamics might also be exploited for extracting metabolic parameters of VOCs on the basis of rebreathing experiments carried out over longer time spans (e.g., several hours, cf. [9]).

A Appendix

This appendix serves to give a roughly self-contained outline of the model structure sketched in Fig. 1. Model equations are derived by taking into account standard conservation of mass laws for the individual compartments. Local diffusion equilibria are assumed to hold at the air-tissue, tissue-blood and air-blood

interfaces, the ratio of the corresponding concentrations being described by the appropriate partition coefficients λ, e.g., $\lambda_{\mathrm{b:air}}$. Unlike for low blood soluble compounds, the amount of highly soluble gas dissolved in the local blood volume of perfused compartments cannot generally be neglected, as it might significantly increase the corresponding capacities. This is particularly true for the airspace compartments. We use the effective compartment volumes $\tilde{V}_{\mathrm{bro}} := V_{\mathrm{bro}} + V_{\mathrm{muc}}\lambda_{\mathrm{muc:air}}$, $\tilde{V}_{\mathrm{A}} := V_{\mathrm{A}} + V_{\mathrm{c'}}\lambda_{\mathrm{b:air}}$, $\tilde{V}_{\mathrm{liv}} := V_{\mathrm{liv}} + V_{\mathrm{liv,b}}\lambda_{\mathrm{b:liv}}$ as well as $\tilde{V}_{\mathrm{tis}} := V_{\mathrm{tis}}$ and neglect blood volumes for the mucosal and tissue compartment. For the bronchial compartment we find that

$$\frac{\mathrm{d}C_{\mathrm{bro}}}{\mathrm{d}t}\tilde{V}_{\mathrm{bro}} = \dot{V}_{\mathrm{A}}(C_{\mathrm{I}} - C_{\mathrm{bro}}) + D(C_{\mathrm{A}} - C_{\mathrm{bro}}) + q_{\mathrm{bro}}\dot{Q}_{\mathrm{c}}\big(C_{\mathrm{a}} - \frac{\lambda_{\mathrm{muc:air}}}{\lambda_{\mathrm{muc:b}}}C_{\mathrm{bro}}\big), \tag{13}$$

with C_{I} denoting the inhaled (ambient) gas concentration, while the mass balance equations for the alveolar, liver and tissue compartment read

$$\frac{\mathrm{d}C_{\mathrm{A}}}{\mathrm{d}t}\tilde{V}_{\mathrm{A}} = D(C_{\mathrm{bro}} - C_{\mathrm{A}}) + (1 - q_{\mathrm{bro}})\dot{Q}_{\mathrm{c}}\big(C_{\bar{\mathrm{v}}} - \lambda_{\mathrm{b:air}}C_{\mathrm{A}}\big), \tag{14}$$

and

$$\frac{\mathrm{d}C_{\mathrm{liv}}}{\mathrm{d}t}\tilde{V}_{\mathrm{liv}} = k_{\mathrm{pr}} - k_{\mathrm{met}}\lambda_{\mathrm{b:liv}}C_{\mathrm{liv}} + q_{\mathrm{liv}}(1 - q_{\mathrm{bro}})\dot{Q}_{\mathrm{c}}\big(C_{\mathrm{a}} - \lambda_{\mathrm{b:liv}}C_{\mathrm{liv}}\big), \tag{15}$$

and

$$\frac{\mathrm{d}C_{\mathrm{tis}}}{\mathrm{d}t}\tilde{V}_{\mathrm{tis}} = (1 - q_{\mathrm{liv}})(1 - q_{\mathrm{bro}})\dot{Q}_{\mathrm{c}}\big(C_{\mathrm{a}} - \lambda_{\mathrm{b:tis}}C_{\mathrm{tis}}\big), \tag{16}$$

respectively. Here,

$$C_{\bar{\mathrm{v}}} := q_{\mathrm{liv}}\lambda_{\mathrm{b:liv}}C_{\mathrm{liv}} + (1 - q_{\mathrm{liv}})\lambda_{\mathrm{b:tis}}C_{\mathrm{tis}} \tag{17}$$

and

$$C_{\mathrm{a}} := (1 - q_{\mathrm{bro}})\lambda_{\mathrm{b:air}}C_{\mathrm{A}} + q_{\mathrm{bro}}\lambda_{\mathrm{muc:air}}C_{\mathrm{bro}}/\lambda_{\mathrm{muc:b}} \tag{18}$$

are the associated concentrations in mixed venous and arterial blood, respectively. Values for the individual compartment volumes and the temperature-dependent partition coefficients are assumed to be known (see Table 3), while cardiac output $\dot{Q}_{\mathrm{c}}$, fractional blood flow to the liver $q_{\mathrm{liv}}(\dot{Q}_{\mathrm{c}})$ (as an empirical function of $\dot{Q}_{\mathrm{c}}$) and alveolar ventilation $\dot{V}_{\mathrm{A}}$ are accessed by direct measurement, see Section 3.1. Within the context of rebreathing experiments, the effective bronchial fractional blood flow q_{bro} is postulated to be represented by a constant nominal value $q_{\mathrm{bro}}^{\mathrm{rest}}$, which generally has to be estimated from experimental data. The same holds true for the initial conditions $\boldsymbol{c}_0 = (C_{\mathrm{bro}}(0), C_{\mathrm{A}}(0), C_{\mathrm{liv}}(0), C_{\mathrm{tis}}(0))$ as well as for the (constant) production and linear metabolism rates k_{pr} and k_{met}, respectively.

Parameter	Symbol	Nominal value (units)
Compartment volumes		
bronchioles	V_{bro}	0.1 (l) [24]
mucosa	V_{muc}	0.005 (l) [24]
alveoli	V_{A}	4.1 (l) [24]
end-capillary	$V_{\mathrm{c}'}$	0.15 (l) [14]
liver	V_{liv}	$0.0285\,\mathrm{LBV}$ (l) [24]
blood liver	$V_{\mathrm{liv,b}}$	1.1 (l) [28]
tissue	V_{tis}	$0.7036\,\mathrm{LBV}$ (l) [24]
Fractional blood flows		
fractional flow bronchioles	q_{bro}	0.01 [21]
fractional flow liver	q_{liv}	0.32 [24]
Partition coefficients at body temperature		
blood:air	$\lambda_{\mathrm{b:air}}$	340 [4, 5]
mucosa:air	$\lambda_{\mathrm{muc:air}}$	392 [19, 32]
blood:liver	$\lambda_{\mathrm{b:liv}}$	1.73 [19]
blood:tissue	$\lambda_{\mathrm{b:tis}}$	1.38 [4]
Metabolic and diffusion constants		
linear metabolic rate	k_{met}	0.0074 ($\mathrm{l/kg^{0.75}/min}$) [18]
endogenous production	k_{pr}	0.19 (mg/min) [18]
stratified conductance	D	0 (l/min) [18]

Table 3: Basic model parameters and nominal values during rest. LBV denotes the lean body volume in liters calculated according to $\mathrm{LBV} = -16.24 + 0.22\,\mathrm{bh} + 0.42\,\mathrm{bw}$, with body height (bh) and weight (bw) given in cm and kg, respectively [24].

References

[1] J. C. Anderson, A. L. Babb, and M. P. Hlastala, *Modeling soluble gas exchange in the airways and alveoli*, Ann Biomed Eng **31** (2003), 1402–22.

[2] J. C. Anderson and M. P. Hlastala, *Breath tests and airway gas exchange*, Pulm Pharmacol Ther **20** (2007), 112–117.

[3] ———, *Impact of Airway Gas Exchange on the Multiple Inert Gas Elimination Technique: Theory.*, Ann Biomed Eng **38** (2010), 1017–1030.

[4] J. C. Anderson, W. J. Lamm, and M. P. Hlastala, *Measuring airway exchange of endogenous acetone using a single-exhalation breathing maneuver*, J Appl Physiol **100** (2006), 880–9.

[5] O. B. Crofford, R. E. Mallard, R. E. Winton, N. L. Rogers, J. C. Jackson, and U. Keller, *Acetone in breath and blood*, Trans Am Clin Climatol Assoc **88** (1977), 128–39.

[6] J. Duffin, R. M. Mohan, P. Vasiliou, R. Stephenson, and S. Mahamed, *A model of the chemoreflex control of breathing in humans: model parameters measurement*, Respir Physiol **120** (2000), 13–26.

[7] L. E. Farhi, *Elimination of inert gas by the lung*, Respiration Physiology **3** (1967), 1–11.

[8] J. G. Filser, *The closed chamber technique – uptake, endogenous production, excretion, steady-state kinetics and rates of metabolism of gases and vapors*, Arch Toxicol **66** (1992), 1–10.

[9] J. G. Filser, G. A. Csanády, B. Denk, M. Hartmann, A. Kauffmann, W. Kessler, P. E. Kreuzer, C. Pütz, J. H. Shen, and P. Stei, *Toxicokinetics of isoprene in rodents and humans*, Toxicology **113** (1996), 278–287.

[10] F. S. Grodins, J. Buell, and A. J. Bart, *Mathematical analysis and digital simulation of the respiratory control system*, J Appl Physiol **22** (1967), 260–76.

[11] E. Hairer, Norsett S. P., and G. Wanner, *Solving ordinary differential equations 1: Nonstiff problems*, 2nd ed., Springer, Berlin, 1993.

[12] L. M. Hanna and P. W. Scherer, *A theoretical model of localized heat and water vapor transport in the human respiratory tract*, J Biomech Eng **108** (1986), 19–27.

[13] S. Huet, A. Bouvier, M.-A. Poursat, and E. Jolivet, *Statistical tools for nonlinear regression*, Springer, New York, 2003.

[14] J. M. B. Hughes and N. W. Morell, *Pulmonary Circulation. From basic mechanisms to clinical practice*, Imperial College Press, London, 2001.

[15] A. W. Jones, *Role of rebreathing in determination of the blood-breath ratio of expired ethanol*, J Appl Physiol **55** (1983), 1237–1241.

[16] M. P. Kalapos, *On the mammalian acetone metabolism: from chemistry to clinical implications*, Biochim Biophys Acta **1621** (2003), 122–39.

[17] J. King, A. Kupferthaler, K. Unterkofler, H. Koc, S. Teschl, G. Teschl, W. Miekisch, J. Schubert, H. Hinterhuber, and A. Amann, *Isoprene and acetone concentration profiles during exercise on an ergometer*, Journal of Breath Research **3** (2009), 027006 (16pp).

[18] J. King, K. Unterkofler, G. Teschl, S. Teschl, H. Hinterhuber, and A. Amann, *A mathematical model for breath gas analysis of volatile organic compounds with special emphasis on acetone*, Preprint.

[19] S. Kumagai and I. Matsunaga, *Physiologically based pharmacokinetic model for acetone*, Occup Environ Med **52** (1995), 344–352.

[20] ———, *A lung model describing uptake of organic solvents and roles of mucosal blood flow and metabolism in the bronchioles*, Inhal Toxicol **12** (2000), 491–510.

[21] A. B. Lumb, *Nunn's applied respiratory physiology*, Butterworth-Heinemann, Oxford, 2005.

[22] R. Mohan and J. Duffin, *The effect of hypoxia on the ventilatory response to carbon dioxide in man*, Respir Physiol **108** (1997), 101–115.

[23] D. E. Mohrman and L. J. Heller, *Cardiovascluar physiology*, 6th ed., Lange Medical Books/McGraw-Hill, New York, 2006.

[24] A. K. Mörk and G. Johanson, *A human physiological model describing acetone kinetics in blood and breath during various levels of physical exercise*, Toxicol Lett **164** (2006), 6–15.

[25] M. E. O'Hara, T. H. Clutton-Brock, S. Green, and C. A. Mayhew, *Endogenous volatile organic compounds in breath and blood of healthy volunteers: examining breath analysis as a surrogate for blood measurements*, Journal of Breath Research **3** (2009), 027005 (10pp).

[26] M. E. O'Hara, S. O'Hehir, S. Green, and C. A. Mayhew, *Development of a protocol to measure volatile organic compounds in human breath: a comparison of rebreathing and on-line single exhalations using proton transfer reaction mass spectrometry*, Physiol Meas **29** (2008), 309–30.

[27] J. Ohlsson, D. D. Ralph, M. A. Mandelkorn, A. L. Babb, and M. P. Hlastala, *Accurate measurement of blood alcohol concentration with isothermal rebreathing*, J Stud Alcohol **51** (1990), 6–13.

[28] J. T. Ottesen, M. S. Olufsen, and J. K. Larsen, *Applied mathematical models in human physiology*, SIAM, Philadelphia, 2004.

[29] K. Schwarz, W. Filipiak, and A. Amann, *Determining concentration patterns of volatile compounds in exhaled breath by PTR-MS*, Journal of Breath Research **3** (2009), 027002 (15pp).

[30] K. Schwarz, A. Pizzini, B. Arendacka, K. Zerlauth, W. Filipiak, A. Schmid, A. Dzien, S. Neuner, M. Lechleitner, S. Scholl-Burgi, W. Miekisch, J. Schubert, K. Unterkofler, V. Witkovsky, G. Gastl, and A. Amann, *Breath acetone – aspects of normal physiology related to age and gender as determined in a PTR-MS study*, Journal of Breath Research **3** (2009), 027003 (9pp).

[31] J. Shao and D. Tu, *The jackknife and bootstrap*, Springer, New York, 1995.

[32] J. Staudinger and P. V. Roberts, *A critical compilation of Henry's law constant temperature dependence relations for organic compounds in dilute aqueous solutions*, Chemosphere **44** (2001), 561–576.

[33] J. B. West, *Respiratory Physiology. The Essentials*, 7th ed., Lippincott Williams & Wilkins, Baltimore, 2005.

[34] E. Wigaeus, S. Holm, and I. Astrand, *Exposure to acetone. Uptake and elimination in man*, Scand J Work Environ Health **7** (1981), 84–94.

[35] A. Zwart, S. C. Luijendijk, and W. R. de Vries, *Excretion-retention data of steady state gas exchange in tidal breathing. I. Dependency on the blood-gas partition coefficient*, Pflügers Arch **407** (1986), 204–210.